Nonlocal Interface Problems: Modeling, Regularity, Finite Element Approximation

Gissell Estrada–Rodriguez* Heiko Gimperlein*† Jakub Stocek*

Abstract

We study interface problems for nonlocal elliptic operators like the fractional Laplacian. We derive relevant strong formulations from microscopic movement models, as relevant to the movement of immune cells in the white and gray matter in the brain. For the resulting problems we obtain precise asymptotic expansions for the behaviour of solutions near the interface, depending on the fractional orders in the neighbouring domains and the diffusion coefficients. The expansions allow to prove optimal convergence rates for finite element approximations on suitably graded meshes. Numerical experiments underline the analysis and show the rich behavior of solutions. This article is the first in a series on the local behavior of solutions near boundaries, interfaces and corner and their numerical approximation.

1 Introduction

Boundary problems for nonlocal elliptic differential equations have attracted much recent interest. In applications, however, interface problems often arise. In solid mechanics, composite bodies lead to interfaces between local and nonlocal material laws [1, 2, 3]. Nonlocal interface problems also arise for optical metamaterials [4], for quasigeostrophic equations in meteorology [5], in shape optimization [6], image processing [7, 8, 9], as well as for biological cell movement [10] and swarm robotic systems [11] in heterogeneous environments.

The local behaviour of solutions to interface problems for elliptic differential operators has been studied for several decades, see e.g. [12, 13, 14]. Explicit singular expansions near the interface allow to devise graded meshes with optimal convergence rates for numerical approximations by finite or boundary elements [12, 15, 16].

In this article we study the singularities and numerical approximation of interface problems for the fractional Laplacian. Because of the nonlocal nature of the operator, the coupling conditions extend across the interface, and their precise nature crucially affects the interface behaviour. We derive a relevant class of model problems from microscopic models for cell movement.

To be specific, for a decomposition of a domain $\overline{\Omega} = \overline{\Omega}_1 \cup \overline{\Omega}_2$ into smooth, disjoint domains as in Figure 1, we consider an interface problem between fractional Laplace-type operators

*Maxwell Institute for Mathematical Sciences and Department of Mathematics, Heriot–Watt University, Edinburgh, EH14 4AS, United Kingdom, email: h.gimperlein@hw.ac.uk.

†Institute for Mathematics, University of Paderborn, Warburger Str. 100, 33098 Paderborn, Germany.

G. E.-R. and J. S. were supported by The Maxwell Institute Graduate School in Analysis and its Applications, a Centre for Doctoral Training funded by the UK Engineering and Physical Sciences Research Council (grant EP/L016508/01), the Scottish Funding Council, Heriot-Watt University and the University of Edinburgh.

corresponding to different orders and different diffusion coefficients in Ω_1 and Ω_2. The precise transmission conditions between the subdomains Ω_1, Ω_2 are contained in the bilinear form (30) below, motivated by the modeling in Section 1.1.

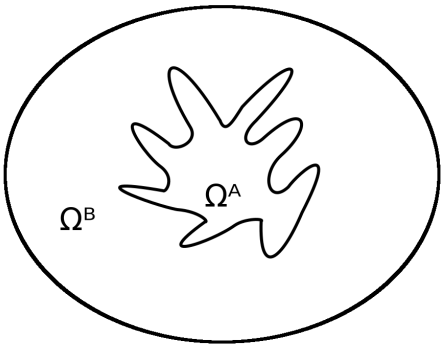

Figure 1: Model geometry for the interface problem

Based on a detailed study of the boundary behaviour using Mellin transform methods, we obtain a precise description of the singular behavior of the solution near $\Gamma = \partial\Omega_1 \cap \Omega_2$. Under mild conditions, the solution admits an asymptotic expansion in Ω_1 and Ω_2 with singular exponents determined by an explicit nonlinear equation (Theorem 4.2).

The precise asymptotic description of the solution has implications for the approximation by finite element methods. We show that algebraically graded meshes adapted to the singularities recover the optimal approximation rates expected for smooth solutions:

Theorem. Let $u \in H(\Omega_1, \Omega_2, s_1, s_2)$ be the solution to the continuous interface problem, u_h the Galerkin approximation to u on a β-graded mesh in $\in \mathbb{V}_h$. Then

$$\|u - u_h\|_{H(\Omega_1,\Omega_2,s_1,s_2)} \lesssim h^{\min\{\beta_1(\nu_1 - s_1 + \frac{1}{2}), \beta_1(\nu_2 - s_2 + \frac{1}{2}), 2 - \max\{s_1, s_2\}\}} |\log^*(h)| \ .$$

Similar results are obtained for a problem which has been of recent interest in shape optimization.

Numerical experiments confirm the theoretical results for the singular exponents and achieve the predicted convergence rates. The convergence rate in the energy norm is doubled when the uniform mesh is replaced by a 2-graded one.

This article is the first in a series on the local behavior of solutions near boundaries corners and their numerical approximation [17].

1.1 Motivation of interface problems in biological movement

Navigation and migration of organisms is directly affected by the physical characteristics of the media. At the level of microorganisms, interactions between cells and the extracellular matrix, a network composed of oriented fibres to which cells attach and migrate, are a key ingredient to understand processes such as wound healing [18, 19]. The extracellular matrix is a heterogeneous medium where fibres align forming different patterns. When migrating cells change from one fibre orientation to another, the interface between these two media alters the velocity and adhesion properties of the cells, and therefore, the overall migration.

Aggregates (overcrowded regions) of microorganisms in different areas are another type of inhomogeneities in the medium that affect the motility of the cells. When migrating cells

encounter an aggregate, they stay trapped for some time, called residence time, resulting in anomalous subdiffusive transport where the mean square displacement of the cells scales like t^μ for $\mu \in (0,1)$ [20]. The anomalous exponent $\mu(x)$ is a function of the space describing long waiting times in crowded areas $\mu \to 0$, or normal diffusion, $\mu \to 1$, for low densities.

The differential movement of T cells in grey and white brain matter [21] provides an instance of interface problems between different substrates. This is directly connected with the intrinsic characteristics of the extracellular matrix in both media. On the other hand, recent experimental observations [22] evidence a change in the search strategy of T cell. In particular, T cells move in an undirected way, describing long trajectories characteristic of nonlocal diffusion (see also [23]). However, once they sense the presence of a tumour, they follow a more localized motion [24]. This switching mechanism shows the presence of an interface at which T cells adaptively change their motion.

The effect of the interface between two different habitats is also observed when larger organisms migrate in heterogeneous media [25, 26]. The movement of a population across two different regions cannot be explained in terms of each media independently, the interface (also referred to as *edge* in this context) provides a new ecological environment not present in either media in isolation.

Analogous to the case of cells migrating in the presence of aggregates, a non-Fickian (anomalous) transport of contaminants was observed in experiments with porous and fractured media (see [27, 28] and references therein). In this case, particles get trapped in stagnation regions which leads to the subdiffusion transport. More generally, due to the heterogeneous nature of geological materials [27], the contaminants experience a wide range of velocities traveling from one medium to another, resulting in anomalous transport.

2 Preliminaries on the fractional Laplacian

In this section we set notation and some properties related to the fractional Laplacian. We focus on the fractional Laplacian $(-\Delta)^s$ with $0 < s < 1$ of a function $u : \mathbb{R}^n \to \mathbb{R}$ given by

$$(-\Delta)^s u(x) = c_{n,s}\, P.V. \int_{\mathbb{R}^n} \frac{u(x) - u(y)}{|x-y|^{n+2s}}\, \mathrm{d}y, \tag{1}$$

where $P.V.$ denotes the Cauchy principle value integral. The normalization constant $c_{n,s}$ is given by

$$c_{n,s} = \frac{2^{2s} s \Gamma\left(\frac{n+2s}{2}\right)}{\pi^{\frac{n}{2}} \Gamma\left(1-s\right)}. \tag{2}$$

Equivalently, the fractional Laplacian can be viewed as an operator with symbol $2s$ or in terms of the Fourier transform $\mathcal{F}((-\Delta)^s u(x)) = |\xi|^{2s} \mathcal{F}u(x)$. Note that one recovers the ordinary Laplacian when $s = 1$.

For a bounded Lipschitz domain $\Omega \subset \mathbb{R}^n$, define the fractional Laplacian to be the restriction of (1) to functions with compact support in Ω.
The Sobolev space $H^s(\Omega)$ associated with the fractional Laplacian is defined by

$$H^s(\Omega) = \{v \in L^2(\Omega) : |v|_{H^s(\Omega)} < \infty\}, \tag{3}$$

where $|\cdot|_{H^s(\Omega)}$ is the Aronszajn-Slobodeckij seminorm

$$|v|^2_{H^s(\Omega)} = \iint_{\Omega\times\Omega} \frac{(v(x)-v(y))^2}{|x-y|^{n+2s}}\, \mathrm{d}y\, \mathrm{d}x. \tag{4}$$

Clearly, $H^s(\Omega)$ is a Hilbert space endowed with the norm

$$\|v\|_{H^s(\Omega)} = \|v\|_{L^2(\Omega)} + |v|_{H^s(\Omega)}. \tag{5}$$

Furthermore, let us consider the space

$$\widetilde{H}^s(\Omega) = \{v \in H^s(\mathbb{R}^n) : \text{supp } v \subset \Omega\}. \tag{6}$$

We denote the dual space of $\widetilde{H}^s(\Omega)$ by $H^{-s}(\Omega)$.

The bilinear form $b(u,v) = \langle (-\Delta)^s u, v\rangle$ associated to the fractional Laplacian in Ω is given by

$$b(u,v) = \frac{c_{n,s}}{2} \iint_{\mathbb{R}^n \times \mathbb{R}^n} \frac{(u(x)-u(y))(v(x)-v(y))}{|x-y|^{n+2s}}\, \mathrm{d}y\, \mathrm{d}x. \tag{7}$$

The bilinear form extends to a continuous and coercive bilinear form on $\widetilde{H}^s(\Omega)$, i.e. there exist $C, \alpha > 0$ such that

$$b(u,v) \leq C\|u\|_{\widetilde{H}^s(\Omega)}\|v\|_{\widetilde{H}^s(\Omega)},$$
$$b(u,u) \geq \alpha \|u\|^2_{\widetilde{H}^s(\Omega)}.$$

The associated operator to b extends $(-\Delta)^s$ to a bounded operator $(-\Delta)^s : \widetilde{H}^s(\Omega) \to H^{-s}(\Omega)$.

The relevant generalization of the normal derivative is now defined for all $x \in \mathbb{R}^n \setminus \Omega$ [29]:

$$\mathcal{N}_s u(x) = c_{n,s} \int_\Omega \frac{u(x)-u(y)}{|x-y|^{n+2s}}\, \mathrm{d}y\,. \tag{8}$$

3 Nonlocal interface problems for biological movement

In this section we derive relevant nonlocal PDE description at the interface. Because of the nonlocal nature of the operator, the coupling between domains extends across the interface, and its precise nature crucially affects the interface behaviour.

Transport equations in heterogeneous environments can be studied in the sense of individuals moving from one habitat to another. The dependence of the medium is introduced via a directional distribution $q(\mathbf{x}, \mathbf{v})$, as proposed in [30], that depends on the transition from one medium to another. In this section we follow some of the assumptions considered in [30].

Let Ω be an open subset of $\mathbb{R}^n$ which decomposes into two disjoint habitats, Ω_A and Ω_B. Consider a population of density $\sigma(\mathbf{x}, t, \mathbf{v}, \tau)$ moving in Ω, where $\mathbf{x} \in \Omega \subset \mathbb{R}^n$, $t \in \mathbb{R}^+$ and $\mathbf{v}$ lies in the unit sphere $S \subset \mathbb{R}^n$ as in previous sections. The particles start at $(\mathbf{x}, t)$ and move in direction $\mathbf{v}$ with fixed speed for some time τ, following a velocity jump process [31].

We define the movement of particles across the interface in terms of a weighting function $W[H(\mathbf{z}), H(\mathbf{y})]$, where $H(\mathbf{y})$ is the current habitat of the particle at position $\mathbf{y}$ and $H(\mathbf{z})$ is the habitat at $\mathbf{z}$, to which the particle moves. For $\mathbf{y} \in \Omega_A$, then $H(\mathbf{y}) = A$ and similarly, for $\mathbf{z} \in \Omega_B$ we have $H(\mathbf{z}) = B$. We define the transition rates:

$$W(A,A) = W(B,B) = 1,\ W(A,B) = a \text{ and } W(B,A) = b. \tag{9}$$

To describe the movement of the particles we have, for $\mathbf{z} = \mathbf{y} + \mathbf{v}\tau$,

$$q(\mathbf{y}, \mathbf{v}) = \mathcal{F}(\mathbf{z}|\mathbf{y}) W[H(\mathbf{z}), H(\mathbf{y})], \tag{10}$$

where $\int_S q(\mathbf{y}, \mathbf{v}) d\mathbf{v} = 1$. $\mathcal{F}$ denotes the probability of running to $\mathbf{z}$ from $\mathbf{y}$ in a time τ in the absence of an interface, while W incorporates the reflection at the interface.

3.1 Transport equation for the simplified interface problem

Near the interface, the movement of a population of density $\sigma(\mathbf{x}, t, \mathbf{v}, \tau)$ can be described by the following transport equation,

$$(\partial_\tau + \partial_t + \mathbf{v} \cdot \nabla)\, \sigma(\cdot, \mathbf{v}, \tau) = -\beta(\mathbf{x}, \tau)\sigma(\cdot, \mathbf{v}, \tau), \tag{11}$$

$$\sigma(\cdot,\mathbf{v},0)=q(\mathbf{x},\mathbf{v})\int_0^t\int_S\beta(\mathbf{x},\tau)\sigma(\cdot,\mathbf{v},\tau)d\mathbf{v}d\tau. \tag{12}$$

where particles at $(\mathbf{x},t)$, denoted by $(\cdot)$, move in direction $\mathbf{v}$ for some time τ. The quantity β, which describes the stopping frequency is given in terms of

$$\psi(\mathbf{x},\tau)=\Big(\frac{\tau_0}{\tau_0+\tau}\Big)^{\alpha(\mathbf{x})}\ , \tag{13}$$

where $\alpha(\mathbf{x})\in(1,2)$ is a space-dependent anomalous exponent. The function $\psi(\mathbf{x},\tau)$ gives the probability that a particle keeps moving for time τ without stopping. Hence, the stopping frequency is given by

$$\beta(\mathbf{x},\tau)=-\frac{\partial_\tau\psi}{\psi}=\frac{\alpha(\mathbf{x})}{\tau_0+\tau}\ . \tag{14}$$

Integrating (11) with respect to τ we obtain

$$\partial_t\bar\sigma+\mathbf{v}\cdot\nabla\bar\sigma=q(\mathbf{x},\mathbf{v})\int_S\int_0^t\beta(\mathbf{x},\tau)\sigma(\cdot,\mathbf{v},\tau)d\tau d\mathbf{v}-\int_0^t\beta(\mathbf{x},\tau)\sigma(\cdot,\mathbf{v},\tau)d\tau. \tag{15}$$

According to [32], we can write the right hand side of (15) in terms of the convolution

$$\int_0^t\beta(\mathbf{x},\tau)\sigma(\cdot,\mathbf{v},\tau)d\tau=\int_0^t\mathcal{B}(\mathbf{x},t-s)\bar\sigma(\mathbf{x}-\mathbf{v}(t-s),\mathbf{v},s)ds.$$

The operator $\mathcal{B}$ is written explicitly in the Laplace space as follows

$$\hat{\mathcal{B}}(\mathbf{x},\lambda+\mathbf{v}\cdot\nabla)=\frac{\hat\varphi(\mathbf{x},\lambda+\mathbf{v}\cdot\nabla)}{\hat\psi(\mathbf{x},\lambda+\mathbf{v}\cdot\nabla)}\ ,$$

where λ is the Laplace variable and $\varphi=-\partial_\tau\psi$. Using a scaling $(\mathbf{x},t,\mathbf{v},\tau)\mapsto(\mathbf{x}/\varepsilon,t/\varepsilon,\mathbf{v}/\varepsilon^\gamma,\tau/\varepsilon^\mu)$, and a quasi-static approximation where $\hat{\mathcal{B}}_\varepsilon(\mathbf{x},\varepsilon\lambda+\varepsilon^{1-\gamma}\mathbf{v}\cdot\nabla)\simeq\hat{\mathcal{B}}_\varepsilon(\mathbf{x},\varepsilon^{1-\gamma}\mathbf{v}\cdot\nabla)$ we write (15) as

$$\begin{aligned}\varepsilon\partial_t\bar\sigma+\varepsilon^{1-\gamma}\mathbf{v}\cdot\nabla\bar\sigma=q(\mathbf{x},\mathbf{v})\int_S\mathcal{B}_\varepsilon(\mathbf{x},\varepsilon^{1-\gamma}\mathbf{v}\cdot\nabla)\bar\sigma(\mathbf{x},t,\mathbf{v})d\mathbf{v}\\-\mathcal{B}_\varepsilon(\mathbf{x},\varepsilon^{1-\gamma}\mathbf{v}\cdot\nabla)\bar\sigma(\mathbf{x},t,\mathbf{v}).\end{aligned} \tag{16}$$

Expanding $\hat{\mathcal{B}}_\varepsilon(\mathbf{x},\varepsilon^{1-\gamma}\mathbf{v}\cdot\nabla)$ using the Laplace transform of ψ and φ [32] and letting the scaling of the run time $\mu=\frac{2-\alpha(\mathbf{x})}{2(\alpha(\mathbf{x})-1)}$ we obtain

$$\begin{aligned}\varepsilon\partial_t\bar\sigma+\varepsilon^{1-\gamma}\mathbf{v}\cdot\nabla\bar\sigma=\varepsilon^{\frac{\alpha(\mathbf{x})-2}{2(\alpha(\mathbf{x})-1)}}\Big[q(\mathbf{x},\mathbf{v})\int_S\frac{\alpha(\mathbf{x})-1}{\tau_0}\bar\sigma(\mathbf{x},t,\mathbf{v})d\mathbf{v}-\frac{\alpha(\mathbf{x})-1}{\tau_0}\bar\sigma(\mathbf{x},t,\mathbf{v})\Big]\\+\varepsilon^{\frac{\alpha(\mathbf{x})-2}{2(\alpha(\mathbf{x})-1)}+\gamma}\Big[-q(\mathbf{x},\mathbf{v})\int_S A(\mathbf{v}\cdot\nabla)^{\alpha(\mathbf{x})-1}\bar\sigma d\mathbf{v}+A(\mathbf{v}\cdot\nabla)^{\alpha(\mathbf{x})-1}\bar\sigma\Big]+\mathcal{O}(\varepsilon^0)\ ,\end{aligned} \tag{17}$$

for $\alpha(\mathbf{x})>3/2$ and $A=\tau_0^{\alpha(\mathbf{x})-2}(1-\alpha(\mathbf{x}))^2\Gamma(-\alpha(\mathbf{x})+1)c_0^{\alpha(\mathbf{x})-1}$.

Substituting the Hilbert expansion $\bar\sigma(\mathbf{x},t,\mathbf{v})=\bar\sigma^0+\varepsilon^\kappa\bar\sigma^\perp+\mathcal{O}(\varepsilon^2)$ and computing the powers of ε we get

$$\bar\sigma^0=q(\mathbf{x},\mathbf{v})u(\mathbf{x},t)\ .$$

The Chapman-Enskog expansion is given by

$$\bar\sigma(\mathbf{x},t,\mathbf{v})=u(\mathbf{x},t)q(\mathbf{x},\mathbf{v})+\varepsilon^\kappa\bar\sigma^\perp(\mathbf{x},t,\mathbf{v})+\mathcal{O}(\varepsilon^2). \tag{18}$$

Hence, integrating (16) with respect to $\mathbf{v}$ and since $\int_S q(\mathbf{x},\mathbf{v})d\mathbf{v}=1$ we get the following conservation equation

$$\varepsilon\partial_t\int_S\bar\sigma d\mathbf{v}+\varepsilon^{1-\gamma}\int_S\mathbf{v}\cdot\nabla\bar\sigma d\mathbf{v}=0. \tag{19}$$

Substituting the expansion of the solution given by (18) into the conservation equation and using the fact that $\int_S \bar{\sigma}^{\perp} d\mathbf{v} = 0$ we have

$$\varepsilon \partial_t u + \varepsilon^{1-\gamma} \nabla \cdot \Big[\mathbb{E}_q u + \varepsilon^{\kappa} \int_S \mathbf{v} \bar{\sigma}^{\perp} d\mathbf{v} \Big] = 0, \tag{20}$$

where

$$\mathbb{E}_q = \int_S \mathbf{v} q d\mathbf{v}. \tag{21}$$

Using the same scaling as in [32] we let $\gamma = \kappa = 1/2$, then the leading order of the conservation equation gives

$$\nabla \cdot \mathbb{E}_q u = 0. \tag{22}$$

The next step is to compute the quantity $\bar{\sigma}^{\perp}$ in order to close the conservation equation (20).

We go back to the transport equation (16) and substitute the expansion for $\bar{\sigma}$. After comparing powers of ε from the left and right hand sides,

$$\bar{\sigma}^{\perp} = \frac{\tau_0}{\alpha(\mathbf{x}) - 1} \Big[-qC \int_S (\mathbf{v} \cdot \nabla)^{\alpha(\mathbf{x})-1} (uq) d\mathbf{v} + C (\mathbf{v} \cdot \nabla)^{\alpha(\mathbf{x})-1} (uq) \Big] \tag{23}$$

where C is given by

$$C = -\frac{\pi \tau_0^{\alpha(\mathbf{x})-1} (\alpha(\mathbf{x}) - 1)}{\sin(\pi \alpha(\mathbf{x})) \Gamma(\alpha(\mathbf{x}))} \frac{(n^2 \nu_1 - |S|)}{|S|(\nu_1 - 1)} \ .$$

Substituting the above expression (23) into (20) and defining $\mathbb{E}'_q = \int_S \mathbf{v}' q(\mathbf{x}, \mathbf{v}') d\mathbf{v}'$, we get

$$\partial_t u = C \nabla \cdot \mathbb{E}'_q \Big[\int_S (\mathbf{v} \cdot \nabla)^{\alpha(\mathbf{x})-1} (qu) d\mathbf{v} \Big] - C \nabla \cdot \Big[\int_S \mathbf{v} (\mathbf{v} \cdot \nabla)^{\alpha(\mathbf{x})-1} (qu) d\mathbf{v} \Big]. \tag{24}$$

Since the above equation is valid close to the interface, we define $S_+ = \{\mathbf{v} \in S : \ \mathbf{n} \cdot \mathbf{v} > 0\}$ and $S_- = \{\mathbf{v} \in S : \ \mathbf{n} \cdot \mathbf{v} < 0\}$, where $\mathbf{n}$ is the normal vector at the interface. Then we can write

$$\int_S (\mathbf{v} \cdot \nabla)^{\alpha(\mathbf{x})-1} q(\mathbf{x}, \mathbf{v}) d\mathbf{v} = \int_{S_+} (\mathbf{v} \cdot \nabla)^{\alpha(\mathbf{x})-1} q_+(\mathbf{x}) d\mathbf{v} + \int_{S_-} (\mathbf{v} \cdot \nabla)^{\alpha(\mathbf{x})-1} q_-(\mathbf{x}) d\mathbf{v} \ . \tag{25}$$

Following the approach in [33] we define a generalized fractional Laplacian as

$$\mathbb{D}_M^{\alpha(\mathbf{x})} f(\mathbf{x}) \coloneqq \nabla \cdot \nabla_M^{\alpha(\mathbf{x})-1} f(\mathbf{x}) = \int_S \mathbf{D}^{\alpha(\mathbf{x})} f(\mathbf{x}) M(d\mathbf{v}), \tag{26}$$

where $\mathbf{D}^{\alpha(\mathbf{x})} = (\mathbf{v} \cdot \nabla)^{\alpha(\mathbf{x})}$ and $M(d\mathbf{v})$ is a positive finite measure. Here the fractional gradient is given as

$$\nabla_M^{\alpha(\mathbf{x})} f(\mathbf{x}) = \int_S \mathbf{v} \mathbf{D}^{\alpha(\mathbf{x})} f(\mathbf{x}) M(d\mathbf{v}) = \int_S \mathbf{v} (\mathbf{v} \cdot \nabla)^{\alpha(\mathbf{x})} f(\mathbf{x}) M(d\mathbf{v}). \tag{27}$$

The measure $M(d\mathbf{v})$ controls the flux of particles in different radial directions [34]. In the case of a homogeneous medium, this measure describes the homogeneous diffusion of particles in every direction, while in the case of heterogeneous medium, $M(d\mathbf{v})$ depends on the direction, giving preference to the direction of the mean flow.

Using the notation above, we can write (24) as

$$\partial_t u = C \nabla \cdot \Big[\mathbb{E}'_q \mathbb{D}_{M_+}^{\alpha(\mathbf{x})-1} q_+ u + \mathbb{E}'_q \mathbb{D}_{M_-}^{\alpha(\mathbf{x})-1} q_- u \Big] - C \Big[\mathbb{D}_{M_+}^{\alpha(\mathbf{x})} q_+ u + \mathbb{D}_{M_-}^{\alpha(\mathbf{x})} q_- u \Big] \tag{28}$$

where $M_+(d\mathbf{v})$ takes values from 0 to π and $M_-(d\mathbf{v})$ from π to 2π. Note that the interface effect is only present in the terms $\mathbb{E}'_q$ and $q_\pm$.

As was shown in [32],

$$\mathbb{D}^{\alpha(\mathbf{x})}_{M_+} f(\mathbf{x}) = \Xi_\alpha (-\Delta_{M_+})^{\alpha/2} f(\mathbf{x})$$

where, in two dimensions, for $1 < \alpha(\mathbf{x}) < 2$,

$$\Xi_\alpha = -2\sqrt{\pi}\cos\left(\frac{\pi\alpha(\mathbf{x})}{2}\right)\frac{\Gamma\left(\frac{\alpha(\mathbf{x})+1}{2}\right)}{\Gamma\left(\frac{\alpha(\mathbf{x})+2}{2}\right)}.$$

Assuming that $\mathbb{E}'_q$ is locally constant in space and using the definitions of fractional Laplacian given in (26) we can write

$$\partial_t u = C(\mathbb{E}'_q - 1)\mathbb{D}^{\alpha}_M(\mathbf{x})uq = 2C\Xi_\alpha(\mathbb{E}'_q - 1)(-\Delta_M)^{\alpha(\mathbf{x})/2}uq \tag{29}$$

where $\mathbb{D}^{\alpha(\mathbf{x})}_M = \mathbb{D}^{\alpha(\mathbf{x})}_{M_+} + \mathbb{D}^{\alpha(\mathbf{x})}_{M_-}$ and $q(\mathbf{x})$ takes values q_+ and q_-, depending on the region that the particle is.

Expression (29) can be finally written as

$$\partial_t u = \mathcal{K}(\mathbb{E}'_q - 1)(-\Delta_M)^{\alpha(\mathbf{x})/2}uq\ ,$$

where $\mathcal{K} = 2C\Xi_\alpha$. Here $\mathcal{K}$, $\mathbb{E}'_q$ and q jump at the interface.

4 Interface problems and numerical approximation

In the case of an interface problem, we consider a decomposition of $\overline{\Omega} = \overline{\Omega}_1 \cup \overline{\Omega}_2$ into smooth, disjoint domains, as depicted in Figure 1. For the analysis we assume that the interface $\Gamma = \partial\Omega_1 \cap \partial\Omega_2 \subset \Omega$, so that the interface does not intersect $\partial\Omega$. The general case leads to corner singularities $\Gamma \cap \partial\Omega$. For the Dirichlet problem for the Laplacian these will be addressed in forthcoming work [17].

The nonlocal diffusion equation (29) points to a definition of a biologically relevant nonlocal interface problem, and in particular to the form of the nonlocal interactions between Ω_1 and Ω_2.

For $D_1, D_2 > 0$, $s_1, s_2 \in (0,1)$, we consider the bilinear form

$$\begin{aligned} a(u,v) =& \frac{D_1\, c_{n,s_1}}{2}\iint_{\Omega_1\times\Omega_1}\frac{(u(x)-u(y))(v(x)-v(y))}{|x-y|^{n+2s_1}}\,\mathrm{dy}\,\mathrm{dx} \\ &+ \frac{D_2\, c_{n,s_2}}{2}\iint_{\Omega_2\times\Omega_2}\frac{(u(x)-u(y))(v(x)-v(y))}{|x-y|^{n+2s_2}}\,\mathrm{dy}\,\mathrm{dx} \\ &+ \nu_1\frac{D_1\, c_{n,s_1}}{2}\iint_{\Omega_1\times\Omega_1^C}\frac{(u(x)-u(y))(v(x)-v(y))}{|x-y|^{n+2s_1}}\,\mathrm{dy}\,\mathrm{dx} \\ &+ \nu_2\frac{D_2\, c_{n,s_2}}{2}\iint_{\Omega_2\times\Omega_2^C}\frac{(u(x)-u(y))(v(x)-v(y))}{|x-y|^{n+2s_2}}\,\mathrm{dy}\,\mathrm{dx}\,. \end{aligned} \tag{30}$$

The maximal domain of the bilinear form in L^2 defines Sobolev spaces

$$H(\Omega_1,\Omega_2,s_1,s_2) = \{v \in L^2(\mathbb{R}^n) : a(v,v) < \infty\ , \text{supp } v \subset \Omega\ \}\ .$$

Functions in $H(\Omega_1,\Omega_2,s_1,s_2)$, in particular, have well-defined restrictions to Γ for $s_1, s_2 > 0$.

For f smooth with supp $\subset \Omega$, we study the time-independent transmission problem:

Find $u \in H(\Omega_1,\Omega_2,s_1,s_2)$, such that for all $v \in H(\Omega_1,\Omega_2,s_1,s_2)$

$$a(u,v) = (f,v)_{L^2(\Omega)}\ .$$

This problem fits into the framework of nonlocal boundary problems in [35], and there exists a unique solution.

For a local–nonlocal coupling corresponding to $s_1 = 1$, $s_2 = s$, the analysis of such interface problems has been considered in [5], motivated by quasigeostrophic equations in meteorology.

Solutions of the fractional Laplace equation are known to have singularities near boundary points. For a smooth boundary, the solution admits an asymptotic expansion with leading behaviour $u(x) \sim \delta(x, \partial\Omega)^s$, where $\delta(x, \partial\Omega)$ denotes the distance to the boundary [36]. For the local–nonlocal problem, [5] has obtained a similar leading behaviour near the interface. For completeness, we recall some key results from [5].

First, for the local regularity it is sufficient to localize near a point on the interface and consider a flat interface $\Gamma = \mathbb{R}^{n-1} \times \{0\}$, the intersections of the halfspaces $\Omega_1 = \mathbb{R}^n_-$, $\Omega_2 = \mathbb{R}^n_+$.

In the local coordinates $x = (x', t) \in \mathbb{R}^{n-1} \times \mathbb{R}$ solutions to the local–nonlocal interface problem satisfy a transmission condition across Γ: There exist $\alpha_0 \in ((2s-1)_+, 2s)$ and M_0 with

$$\lim_{t \to 0^-} \frac{u(x', 0) - u(x', t)}{t^{\alpha_0 + 2 - 2s}} = M_0 \lim_{t \to 0^+} \frac{u(x', 0) - u(x', t)}{t^{\alpha_0}}.$$

The existence of the limits is a main result:

Theorem 4.1 (special case of Theorem 7.11, [5]). *Let $f \in C_c^\infty(\Omega)$ and $u \in C^{0,\alpha_*}$ a solution to the interface problem (30), with $s_1 = 1$, $s_2 = s$. Furthermore, assume that $\partial_{e_i} u \in C^{0,\alpha_*}$ for $i \neq n$, and wlog $u = 0$ on Γ. Then there exists $\ell \in \mathbb{R}$ such that*

$$u(x', t) = \ell \left[\rho_{\alpha_0}(t) + M_0 \rho_{\alpha_0 + 2 - 2s}(-t)\right] (1 + q(x)), \tag{31}$$

where $|q(x)| \leq C|x|^\beta$ for some C, β independent of u.

Here,

$$\rho_\lambda(t) = \mathbf{1}_{\{t \geq 0\}} |t|^\lambda. \tag{32}$$

The argument can be extended to give a full asymptotic expansion for the solution u.

In the next sections we determine the asymptotic behavior of solutions for the general nonlocal–nonlocal interface problem.

Theorem 4.2. *Let $f \in C_c^\infty(\Omega)$ and $u \in C^{0,\alpha_*}$ a solution to the interface problem (30). Furthermore, assume that $\partial_{e_i} u \in C^{0,\alpha_*}$ for $i \neq n$, and wlog $u = 0$ on Γ. Then there exist $\mathbf{M}_1$ and $\mathbf{M}_2$ such that*

$$u(x', t) = \left(\mathbf{M}_1 \rho_\alpha(-t) + \mathbf{M}_2 \rho_\beta(t)\right) (1 + q(x)), \tag{33}$$

where $|q(x)| \leq C|x|^\sigma$, for some C, σ independent of u. The exponents α, β are determined as the zeros of an explicit nonlinear function (35):

$$0 = \det \begin{pmatrix} A_{1,1} & A_{1,2} \\ A_{2,1} & A_{2,2} \end{pmatrix}, \qquad A_{i,j} = A_{i,j}(\nu^1, \nu^2, D_1, D_2, s_1, s_2, n) \ .$$

The exponents α, β will be explicitly computed below. The argument can be extended to give a full asymptotic expansion for the solution u.

The asymptotic expansion of the solution has implications for the approximation by finite element methods.

For the numerical approximation, without loss of generality we assume that Ω has a polygonal boundary. Let $\mathcal{T}_h$ be a family of shape-regular triangulations of Ω and $\mathbb{V}_h \subset H(\Omega_1, \Omega_2, s_1, s_2)$, the associated space of continuous piecewise linear functions on $\mathcal{T}_h$, vanishing at the boundary.

The discretized problem is given by:

Find $u_h \in \mathbb{V}_h$, such that for all $v \in \mathbb{V}_h$

$$a(u,v) = (f,v)_{L^2(\Omega)} \ .$$

By coercivity, there exists a unique solution.

Theorem 4.2 implies optimal approximation properties on graded meshes. To define a β-graded mesh on a square or a disc, it suffices to consider β-graded meshes on the unit interval $[-1,0]$. For the square, we consider $x_k = y_k = -1 + (\frac{k}{N})^\beta$ for $k = 1,\dots,N$ and the grading parameter $\beta \geq 1$. The nodes of the β-graded mesh on a square are then given by (x_k, y_ℓ), for $k,\ell = 1,\dots,N$. Note that for $\beta = 1$ we obtain an uniform mesh.
On a disc, to obtain β-graded mesh, the radii r_k are shifted towards the interface and the boundary. In particular, for Ω_1 the radii are given by $r_k = \frac{1}{2}\left(1 - (\frac{k}{N_i})^\beta\right)$, for Ω_2 we grade towards the interface using radii $r_\ell = \frac{1}{2}\left(1 + (\frac{\ell}{N_e})^\beta\right)$ and towards the boundary using radii $r_m = 1 - (\frac{m}{N_b})^\beta$ where the values of N_i, N_e, N_b are chosen appropriately. Eventhough the triangles become increasingly narrower towards the interface and the boundary, their total number stays proportional to N^2.
Examples of 2-graded meshes are depicted in Figure 2.

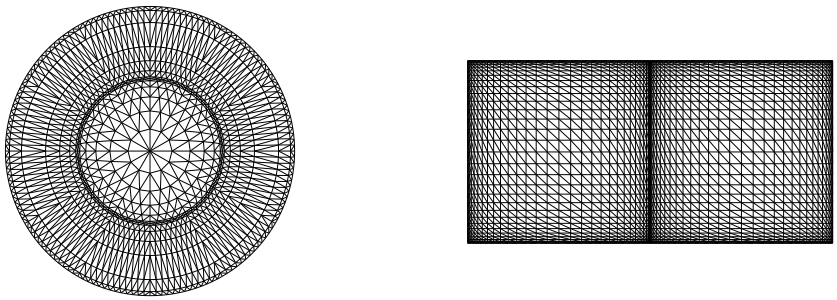

Figure 2: β-graded meshes with $\beta = 2$ for the unit disc and two squares.

Recall the following result from [37, Satz 3.10].

Lemma 4.3. *For $a > 0$ and $s \in [0, a + \frac{1}{2})$ there holds with the linear interpolant $\Pi_y^1 y^a$ of y^a*

$$\|y^a - \Pi_y^1 y^a\|_{\widetilde{H}^s([0,1])} \lesssim h^{\min\{\beta(a-s+\frac{1}{2})-\varepsilon, 2-s\}}.$$

One easily deduces:

Theorem 4.4. *Let $u \in H(\Omega_1,\Omega_2,s_1,s_2)$ be the solution to the continuous interface problem, u_h the Galerkin approximation to u on a β-graded mesh in $\in \mathbb{V}_h$. Then*

$$\|u - u_h\|_{H(\Omega_1,\Omega_2,s_1,s_2)} \lesssim h^{\min\{\beta(\nu_1-s_1+\frac{1}{2}),\beta(\nu_2-s_2+\frac{1}{2}),2-\max\{s_1,s_2\}\}} |\log^*(h)| \ .$$

5 Derivation of asymptotic expansion

In this section we derive the asymptotic expansion of the solution u to the nonlocal–nonlocal interface problem given by the bilinear form (30). For calculations, note that (30) may be

written as

$$
\begin{aligned}
a(u,v) =& D_1\, c_{n,s_1} \iint_{\Omega_1\times\Omega_1} v(x)\frac{(u(x)-u(y))}{|x-y|^{n+2s_1}}\,\mathrm{dy}\,\mathrm{dx} + D_2\, c_{n,s_2} \iint_{\Omega_2\times\Omega_2} v(x)\frac{(u(x)-u(y))}{|x-y|^{n+2s_2}}\,\mathrm{dy}\,\mathrm{dx}\\
&+ \nu_1\,\frac{D_1\, c_{n,s_1}}{2} \iint_{\Omega_1\times\Omega_1^C} v(x)\frac{(u(x)-u(y))}{|x-y|^{n+2s_1}}\,\mathrm{dy}\,\mathrm{dx} + \nu_1\,\frac{D_1\, c_{n,s_1}}{2} \iint_{\Omega_1^C\times\Omega_1} v(x)\frac{(u(x)-u(y))}{|x-y|^{n+2s_1}}\,\mathrm{dy}\,\mathrm{dx}\\
&+ \nu_2\,\frac{D_2\, c_{n,s_2}}{2} \iint_{\Omega_2\times\Omega_2^C} v(x)\frac{(u(x)-u(y))}{|x-y|^{n+2s_2}}\,\mathrm{dy}\,\mathrm{dx} + \nu_2\,\frac{D_2\, c_{n,s_2}}{2} \iint_{\Omega_2^C\times\Omega_2} v(x)\frac{(u(x)-u(y))}{|x-y|^{n+2s_2}}\,\mathrm{dy}\,\mathrm{dx}\\
=& D_1 \int_{\Omega_1} v(x)(-\Delta)^{s_1}u(x)\,\mathrm{dx} + D_2 \int_{\Omega_2} v(x)(-\Delta)^{s_2}u(x)\,\mathrm{dx}\\
&+ \left(\frac{\nu_1}{2}-1\right) D_1\, c_{n,s_1} \iint_{\Omega_1\times\Omega_1^C} v(x)\frac{(u(x)-u(y))}{|x-y|^{n+2s_1}}\,\mathrm{dy}\,\mathrm{dx}\\
&+ \left(\frac{\nu_2}{2}-1\right) D_2\, c_{n,s_2} \iint_{\Omega_2\times\Omega_2^C} v(x)\frac{(u(x)-u(y))}{|x-y|^{n+2s_2}}\,\mathrm{dy}\,\mathrm{dx}\\
&+ \nu_1\,\frac{D_1\, c_{n,s_1}}{2} \iint_{\Omega_2\times\Omega_1} v(x)\frac{(u(x)-u(y))}{|x-y|^{n+2s_1}}\,\mathrm{dy}\,\mathrm{dx} + \nu_2\,\frac{D_2\, c_{n,s_2}}{2} \iint_{\Omega_1\times\Omega_2} v(x)\frac{(u(x)-u(y))}{|x-y|^{n+2s_2}}\,\mathrm{dy}\,\mathrm{dx}\,.
\end{aligned}
$$

The first two terms account for the full fractional Laplacian in Ω_1, Ω_2 separately, while the remaining terms are to be understood as a type of nonlocal transmission terms.
We employ the Mellin transform to determine the local behavior of solutions to the interface problem defined by (30). The Mellin transform corresponds to applying the nonlocal operator to the function $\rho_\lambda(t) = \mathbf{1}_{\{t\geq 0\}}|t|^\lambda$. For the ease of presentation we first compute integrals that arise from applying of the fractional Laplacian to $\rho_\lambda(t)$.
For any $x_n > 0$ we have:

$$
\begin{aligned}
I_1(\sigma,s) := \int_0^\infty \frac{|x_n|^\sigma - |y_n|^\sigma}{|x_n-y_n|^{1+2s}}\,\mathrm{dy}_n &= |x_n|^{\sigma-2s}\int_0^\infty \frac{1-y_n^\sigma}{|1-y_n|^{1+2s}}\,\mathrm{dy}_n\\
&= |x_n|^{\sigma-2s}\left(-\frac{1}{2s} + \frac{\sin(\pi(s-\alpha))}{\sin(\pi s)}\mathbf{B}(\sigma+1,2s-\sigma)\right)
\end{aligned}
$$

For $x_n < 0$ we have:

$$
\begin{aligned}
I_2(\sigma,s) := \int_0^\infty \frac{|x_n|^\sigma}{|x_n-y_n|^{1+2s}}\,\mathrm{dy}_n &= |x_n|^{\sigma-2s}\int_0^\infty \frac{1}{|1+y_n|^{1+2s}}\,\mathrm{dy}_n\\
&= |x_n|^{\sigma-2s}\frac{1}{2s}
\end{aligned}
$$

For $x_n < 0$ we have:

$$
\begin{aligned}
I_3(\sigma,s) := \int_0^\infty \frac{|y_n|^\sigma}{|x_n-y_n|^{1+2s}}\,\mathrm{dy}_n &= |x_n|^{\sigma-2s}\int_0^\infty \frac{y_n^\sigma}{|1+y_n|^{1+2s}}\,\mathrm{dy}_n\\
&= |x_n|^{\sigma-2s}\mathbf{B}(\sigma+1,2s-\sigma).
\end{aligned}
$$

We also define the following quantities:

$$
C(n,s) := \int_{\mathbb{R}^{n-1}} \frac{\mathrm{dy}}{(1+|y|^2)^{\frac{n+2s}{2}}} = \frac{\pi^{\frac{n-1}{2}}\Gamma(s+\frac{1}{2})}{\Gamma(s+\frac{n}{2})},
$$

$$
\begin{aligned}
q(s,\alpha) := \int_0^\infty \frac{1-x^\alpha}{|1-x|^{1+2s}}\,\mathrm{dx} + \int_0^\infty \frac{1}{(1+x)^{1+2s}}\,\mathrm{dx} &= \frac{\Gamma(2\,s-\alpha)\,\Gamma(1+\alpha)\sin(\pi\,(s-\alpha))}{\Gamma(1+2\,s)\sin(\pi\,s)}\\
&= \mathbf{B}(\alpha+1,2s-\alpha)\frac{\sin(\pi\,(s-\alpha))}{\sin(\pi\,s)}.
\end{aligned}
$$

Note that $I_1(\sigma,s)+I_2(\sigma,s)=q(s,\alpha)|x_n|^{\sigma-2s}$.

In order to construct a solution of the interface problem (**??**), we define a one dimensional function

$$v_0(x',x_n)=\mathbf{M}_1\rho_\alpha(-x_n)+\mathbf{M}_2\rho_\beta(x_n),$$

as we expect different singular order near the interface Γ in the respective domains Ω_1,Ω_2. Below we apply the operators corresponding to all the terms of the bilinear form (**??**).

For any point $x\in\Omega_1$, that is $x_n<0$, from applying the fractional Laplacian to $v_0(x)$ we obtain

$$\begin{aligned}D_1\,(-\Delta)^{s_1}v_0(x',x_n)&=\mathbf{M}_1\,D_1\,c_{n,s_1}\int_{\mathbb{R}^n}\frac{\rho_\alpha(-x_n)-\rho_\alpha(-y_n)}{|x-y|^{n+2s_1}}\,\mathrm{dy}+\mathbf{M}_2\,D_1\,c_{n,s_1}\int_{\mathbb{R}^n}\frac{\rho_\beta(x_n)-\rho_\beta(y_n)}{|x-y|^{n+2s_1}}\,\mathrm{dy}\\&=\mathbf{M}_1\,D_1\,c_{n,s_1}\,C(n,s_1)\,(I_1(\alpha,s_1)+I_2(\alpha,s_1))-\mathbf{M}_2\,D_1\,c_{n,s_1}\,C(n,s_1)\,I_3(\beta,s_1)\\&=\mathbf{M}_1\,D_1c_{n,s_1}C(n,s_1)q(\alpha,s_1)|x_n|^{\alpha-2s_1}-\mathbf{M}_2D_1c_{n,s_1}C(n,s_1)\mathbf{B}(\beta+1,2s_1-\beta)|x_n|^{\beta-2s_1}.\end{aligned}$$

Furthermore, the transmission terms with $x\in\Omega_1$ give

$$\begin{aligned}\left(\frac{\nu_1}{2}-1\right)\,D_1\,c_{n,s_1}\int_{\Omega_2}\frac{v_0(x)-v_0(y)}{|x-y|^{n+2s_1}}\,\mathrm{dy}&=\left(\frac{\nu_1}{2}-1\right)\,D_1\,c_{n,s_1}C(n,s_1)\,(\mathbf{M}_1\,I_2(\alpha,s_1)-\mathbf{M}_2I_3(\beta,s_1))\\&=\left(\frac{\nu_1}{2}-1\right)\,D_1\,c_{n,s_1}C(n,s_1)\left(\mathbf{M}_1\frac{1}{2s_1}|x_n|^{\alpha-2s_1}-\mathbf{M}_2\mathbf{B}(\beta+1,2s_1-\beta)|x_n|^{\beta-2s_1}\right),\end{aligned}$$

and

$$\begin{aligned}\frac{\nu_2}{2}\,D_2\,c_{n,s_2}\int_{\Omega_2}\frac{v_0(x)-v_0(y)}{|x-y|^{n+2s_2}}\,\mathrm{dy}&=\frac{\nu_2}{2}\,D_2\,c_{n,s_2}C(n,s_2)\,(\mathbf{M}_1I_2(\alpha,s_2)-\mathbf{M}_2I_3(\beta,s_2))\\&=\frac{\nu_2}{2}\,D_2\,c_{n,s_2}C(n,s_2)\left(\mathbf{M}_1\,\frac{1}{2s_2}|x_n|^{\alpha-2s_2}-\mathbf{M}_2\,\mathbf{B}(\beta+1,2s_2-\beta)|x_n|^{\beta-2s_2}\right).\end{aligned}$$

Behaviour of the function $v_0(x)$ for any $x\in\Omega_2$, that is $x_n>0$, can be obtained in the same way as for Ω_1.

$$\begin{aligned}D_2\,(-\Delta)^{s_2}v_0(x',x_n)&=\mathbf{M}_1\,D_2\,c_{n,s_2}\int_{\mathbb{R}^n}\frac{\rho_\alpha(-x_n)-\rho_\alpha(-y_n)}{|x-y|^{n+2s_2}}\,\mathrm{dy}+\mathbf{M}_2\,D_2\,c_{n,s_2}\int_{\mathbb{R}^n}\frac{\rho_\beta(x_n)-\rho_\beta(y_n)}{|x-y|^{n+2s_2}}\,\mathrm{dy}\\&=-\mathbf{M}_1\,D_2c_{n,s_2}C(n,s_2)\mathbf{B}(\alpha+1,2s_2-\alpha)|x_n|^{\alpha-2s_2}+\mathbf{M}_2\,D_2c_{n,s_2}C(n,s_2)q(\beta,s_2)|x_n|^{\beta-2s_2},\end{aligned}$$

Similarly the transmission terms for $x\in\Omega_2$ give

$$\left(\frac{\nu_2}{2}-1\right)\,D_2\,c_{n,s_2}\int_{\Omega_1}\frac{v_0(x)-v_0(y)}{|x-y|^{n+2s_2}}\,\mathrm{dy}=\left(\frac{\nu_2}{2}-1\right)\,D_2\,c_{n,s_2}C(n,s_2)\left(-\mathbf{M}_1\,\mathbf{B}(\alpha+1,2s_2-\alpha)|x_n|^{\alpha-2s_2}+\mathbf{M}_2\frac{1}{2s_2}|x_n|^{\beta-2s_2}\right),$$

and

$$\frac{\nu_1}{2}\,D_1\,c_{n,s_1}\int_{\Omega_1}\frac{v_0(x)-v_0(y)}{|x-y|^{n+2s_1}}\,\mathrm{dy}=\frac{\nu_1}{2}\,D_1\,c_{n,s_1}C(n,s_1)\left(-\mathbf{M}_1\mathbf{B}(\alpha+1,2s_1-\alpha)|x_n|^{\alpha-2s_1}+\mathbf{M}_2\frac{1}{2s_1}|x_n|^{\beta-2s_1}\right).$$

We define

$$\begin{aligned}\mathcal{Q}(s_i,\sigma)&=c_{n,s_i}C(n,s_i)q(\sigma,s_i)|x_n|^{\sigma-2s_i},\\\mathcal{S}(s_i,\sigma,\nu_j)&=\frac{\nu_j}{2}c_{n,s_i}C(n,s_i)\frac{1}{2s_i}|x_n|^{\sigma-2s_i},\\\mathcal{B}(s_i,\sigma,\nu_j)&=-\frac{\nu_j}{2}c_{n,s_i}C(n,s_i)\mathbf{B}(\sigma+1,2s_i-\sigma)|x_n|^{\sigma-2s_i},\end{aligned}$$

and by collecting terms in Ω_1, respectively Ω_2 obtain the following system

$$\mathbf{A}\begin{pmatrix}\mathbf{M}_1\\ \mathbf{M}_2\end{pmatrix} = \begin{pmatrix}0\\0\end{pmatrix}, \tag{34}$$

where

$$\mathbf{A} = \begin{pmatrix} D_1\,\mathcal{Q}(s_1,\alpha) + D_1\,\mathcal{S}(s_1,\alpha,\nu_1-2) + D_2\,\mathcal{S}(s_2,\alpha,\nu_2) & D_1\,\mathcal{B}(s_1,\beta,\nu_1) + D_2\,\mathcal{B}(s_2,\beta,\nu_2) \\ D_1\,\mathcal{B}(s_1,\alpha,\nu_1) + D_2\,\mathcal{B}(s_2,\alpha,\nu_2) & D_2\,\mathcal{Q}(s_2,\beta) + D_2\,\mathcal{S}(s_2,\beta,\nu_2-2) + D_1\,\mathcal{S}(s_1,\beta,\nu_1)\end{pmatrix}.$$

The asymptotic behaviour of solution u near the interface Γ in Ω_1, Ω_2 can be determined by understanding the leading order singularities of the following:

$$\det \mathbf{A} = 0. \tag{35}$$

6 Singular exponents of specific interface problems

We will now investigate different interface problems for different values of s_1, s_2 and diffusion coefficients D_1, D_2 in the following examples below.

6.1 Local–nonlocal problem

We begin by reproducing the local–nonlocal problem from [5]. To do so, we set $s_1 = 1$. The bilinear form has to be interpreted in the limit as $s_1 \to 1$. In this case the transmission terms from containing ν_1 (terms 3, 5) reduce to the normal derivatives on Γ with the opposite sign, see for example [29]. The bilinear form (30) then reduces to

$$\begin{aligned} a(u,v) &= D_1 \int_{\Omega_1} \nabla u \cdot \nabla v \,\mathrm{dx} + a_{s_2}^{\Omega_2}(u,v) \\ &= \int_{\Omega_1} \nabla u \cdot \nabla v \,\mathrm{dx} + \frac{D_2\ \nu_2\ c_{n,s_2}}{2} \iint_{Q_2} \frac{(u(x)-u(y))(v(x)-v(y))}{|x-y|^{n+2s_2}} \,\mathrm{dy\,dx}, \end{aligned} \tag{36}$$

where $Q_2 = (\Omega_2 \times \mathbb{R}^n) \cup (\mathbb{R}^n \times \Omega_2)$.

The system corresponding to the leading order asymtotic behaviour is given by

$$\begin{aligned} &\mathbf{M}_1(D_1\tilde{C}|x_n|^{\alpha-2} + D_2\mathcal{S}(s_2,\alpha,\nu_2)) + \mathbf{M}_1 D_2\mathcal{B}(s_2,\beta,\nu_2) = 0, \\ &\mathbf{M}_1 D_2\mathcal{B}(s_2,\alpha,\nu_2) + \mathbf{M}_2 D_2(\mathcal{Q}(s_2,\beta) + \mathcal{S}(s_2,\beta,\nu_2-2)) = 0. \end{aligned}$$

Since $s_2 < s_1 = 1$ we expect $\alpha > \beta$. As terms involving $\beta - 2$ are absent from the system, the singular behaviour is determined by terms $\alpha - 2$, $\beta - 2s_2$. When we let $\alpha = \beta + 2 - 2s_2$, the terms involving $\beta - 2s_2$ and $\alpha - 2$ are of the same order and determine the singular behaviour of solutions near the interface. Then the matrix $\mathbf{A}$ reduces to

$$\det \begin{pmatrix} D_1\tilde{C} & -\frac{\nu_2}{2}\,D_2 c_{n,s_2} C(n,s_2)\mathbf{B}(\beta+1, 2s_2-\beta) \\ 0 & D_2 c_{n,s_2} C(n,s_2)(q(\beta,s_2) + (\frac{\nu_2}{2}-1)\frac{1}{2s_2}) \end{pmatrix} = 0.$$

This system has a nontrivial solution precisely when

$$q(\beta,s_2) + (\tfrac{\nu_2}{2}-1)\tfrac{1}{2s_2} = 0,$$

in agreement with [5]. In particular, when $\nu_2 = 2$, the condition reduces to $q(\beta,s_2) = 0$, which is true precisely when $\beta = s_2$ and $\alpha = 2 - s_2$.

6.2 Nonlocal–nonlocal problem involving one sided transmission

Secondly, we investigate the case of one sided transmission mentioned in [5]. We set the transmission terms involving $\nu_1 = 0$. Then the system reduces to

$$\mathbf{M}_1 \left(D_1 \left(\mathcal{Q}(s_1, \alpha) - \mathcal{S}(s_1, \alpha, 2) \right) + D_2 \mathcal{S}(s_2, \alpha, \nu_2) \right) + \mathbf{M}_2 D_2 \mathcal{B}(s_2, \beta, \nu_2) = 0,$$

$$\mathbf{M}_1 D_2 \mathcal{B}(s_2, \alpha, \nu_2) + \mathbf{M}_2 D_2 \left(\mathcal{Q}(s_2, \beta) + \mathcal{S}(s_2, \beta, \nu_2 - 2) \right) = 0.$$

Provided that $s_1 > s_2$ and similarly as in Subsection 6.1 let $\alpha = \beta + 2s_1 - 2s_2$, we obtain

$$\det \begin{pmatrix} D_1 c_{n,s_1} C(n, s_1) \left(q(\alpha, s_1) - \frac{1}{2s_1} \right) & -\frac{\nu_2}{2} D_2 \, c_{n,s_2} C(n, s_2) \mathbf{B}(\beta + 1, 2s_2 - \beta) \\ 0 & D_2 c_{n,s_2} C(n, s_2) \left(q(\beta, s_2) + \left(\frac{\nu_2}{2} - 1 \right) \frac{1}{2s_2} \right) \end{pmatrix} = 0.$$

The only option for nontrivial solution is obtained when $q(\beta, s_2) + \left(\frac{\nu_2}{2} - 1 \right) \frac{1}{2s_2} = 0$, in line with observations in [5].

6.3 Nonlocal–nonlocal problem with distinct diffusion coefficients

Next we investigate the case of different diffusion coefficients. To that end we set the fractional powers to $s_1 = s_2 = s$. By symmetry of the problem we expect $\alpha = \beta$. Then the problem reduces to the following system of equations:

$$\det \begin{pmatrix} D_1 \left(q(\alpha, s) + \frac{\nu_1 - 2}{4s} \right) + D_2 \frac{\nu_2}{4s} & -\left(\frac{D_1 \nu_1 + D_2 \nu_2}{2} \right) \mathbf{B}(\alpha + 1, 2s - \alpha) \\ -\left(\frac{D_1 \nu_1 + D_2 \nu_2}{2} \right) \mathbf{B}(\alpha + 1, 2s - \alpha) & D_2 \left(q(\alpha, s) + \frac{\nu_2 - 2}{4s} \right) + D_1 \frac{\nu_1}{4s} \end{pmatrix} = 0.$$

This suggests a dependency of solutions on both sides of the interface on both D_1, D_2 and is in good agreement with numerical results, see Section 9.

In the case of equal diffusion coefficients $D_1 = D_2 = 1$ and equal transmission $\nu_1 = \nu_2 = 1$ one obtains the following condition for nontrivial solutions of the system:

$$\left(q(\alpha, s) + \mathbf{B}(\alpha + 1, 2s - \alpha) \right) \left(q(\alpha, s) - \mathbf{B}(\alpha + 1, 2s - \alpha) \right) = 0.$$

This has solutions precisely when $\alpha \in (2s - 1)_+ \cup \mathbb{N}$.

6.4 Interface problem arising in shape optimization

Here we discuss a related fractional interface problem as used in shape optimization e.g. in [6]. It corresponds to the bilinear form on $V^{s_1} \cap V^{s_2}$

$$a(u, v) = \frac{1}{2} \iint_{\mathbb{R}^n \times \mathbb{R}^n} \left(v(x) - v(y) \right) \left(u(x) K(x, y) - u(y) K(y, x) \right) \mathrm{d}y \, \mathrm{d}x \,. \tag{37}$$

Here $K(x, y)$ is given by

$$K(x, y) = \begin{cases} D_1 \, c_{n,s_1} \, |x - y|^{-n - 2s_1} & \text{when } x \in \Omega_1 \\ D_2 \, c_{n,s_2} \, |x - y|^{-n - 2s_2} & \text{when } x \in \Omega_2 \\ 0 & \text{when x} \notin \Omega_1 \cup \Omega_2 \end{cases} .$$

The bilinear form can be rewritten into the following form

$$\begin{aligned} a(u, v) = &\iint_{\Omega_1 \times \Omega_1} v(x) \left(u(x) - u(y) \right) K(x, y) \, \mathrm{d}y \, \mathrm{d}x + \iint_{\Omega_2 \times \Omega_2} v(x) \left(u(x) - u(y) \right) K(x, y) \, \mathrm{d}y \, \mathrm{d}x \\ &+ \iint_{\Omega_1 \times \Omega_2} v(x) \left(u(x) K(x, y) - u(y) K(y, x) \right) \mathrm{d}y \, \mathrm{d}x + \iint_{\Omega_2 \times \Omega_1} v(x) \left(u(x) K(x, y) - u(y) K(y, x) \right) \mathrm{d}y \, \mathrm{d}x \,. \end{aligned}$$

Note that the first and second term are the regional contributions of the fractional Laplacian from Ω_1 and Ω_2, respectively. Third and fourth term are to be understood as a transmission condition between Ω_1 and Ω_2. Physically it corresponds to ... ???
The behaviour of solutions near the interface may be studied using techniques of Section **??**. The singular exponents are determined by the solutions to

$$\det \begin{pmatrix} D_1\mathcal{Q}(s_1,\alpha) & D_2\mathcal{B}(s_2,\beta,2) \\ D_1\mathcal{B}(s_1,\alpha,2) & D_2\mathcal{Q}(s_2,\beta) \end{pmatrix} = 0.$$

By symmetry we assume that $s_1 \geq s_2$ and that $\alpha \geq \beta$. As terms involving $\beta - 2s_1$ are absent, the system has nontrivial solution when $\alpha - 2s_1 = \beta - 2s_2$. Equivalently

$$q(\beta + 2s_1 - 2s_2, s_1)q(\beta, s_2) - \mathbf{B}(\beta + 2s_1 - 2s_+1, 2s_2 - \beta)\mathbf{B}(\beta + 1, 2s_2 - \beta) = 0.$$

Note that the condition is independent of D_1, D_2. Recalling the definition of $q(\sigma, s)$ in (**??**) the condition above simplifies into

$$\mathbf{B}(\beta + 2s_1 - 2s_2 + 1, 2s_2 - \beta)\mathbf{B}(\beta + 1, 2s_2 - \beta)\left(\frac{\sin(\pi(2s_2 - s_1 - \beta))\sin(\pi(s_2 - \beta))}{\sin(\pi s_1)\sin(\pi s_2)} - 1\right) = 0,$$

and as $\mathbf{B}(\cdot,\cdot) > 0$, the singular term β is determined by

$$\frac{\sin(\pi(\beta - 2s_2))\sin(\pi(\beta + s_1 - s_2))}{\sin(\pi s_1)\sin(\pi s_2)} = 0.$$

We conclude that

$$\beta \in (2s_2 + \mathbb{Z}) \cup (s_2 - s_1 + \mathbb{Z}) \text{ and } \alpha \in (2s_1 + \mathbb{Z}) \cup (s\_1 - s_2 + \mathbb{Z})$$

The value of $\beta \in ((2s_2 - 1)_+, 2s_2)$, therefore the only possible value of the leading order singularity is $\beta = 1 - s_1 + s_2$, provided $s_1 + s_2 > 1$.

7 Algorithmic aspects

We implement the bilinear form $a(\cdot,\cdot)$ associated with the interface problem for the fractional Laplacian in $\widetilde{\mathbb{V}}_h = \mathbb{S}^1(\mathcal{T}_h) \cap H^s_0(\Omega)$ similarly as described in [38, 39, 40]. In the nodal basis $\{\phi_i\}$ of $\mathbb{V}_h$ the stiffness matrix $K = (K_{ij})$ is given by

$$\begin{aligned} K_{ij} = a(\phi_i, \phi_j) =& \frac{D_1\, c_{n,s_1}}{2} \iint_{\Omega_1\times\Omega_1} \frac{(\phi_i(x) - \phi_i(y))(\phi_j(x) - \phi_j(y))}{|x-y|^{n+2s_1}}\,\mathrm{dy}\,\mathrm{dx} \\ &+ \frac{D_2\, c_{n,s_2}}{2} \iint_{\Omega_2\times\Omega_2} \frac{(\phi_i(x) - \phi_i(y))(\phi_j(x) - \phi_j(y))}{|x-y|^{n+2s_2}}\,\mathrm{dy}\,\mathrm{dx} \\ &+ \nu_1 \frac{D_1\, c_{n,s_1}}{2} \iint_{\Omega_1\times\Omega_1^C} \frac{(\phi_i(x) - \phi_i(y))(\phi_j(x) - \phi_j(y))}{|x-y|^{n+2s_1}}\,\mathrm{dy}\,\mathrm{dx} \\ &+ \nu_2 \frac{D_2\, c_{n,s_2}}{2} \iint_{\Omega_2\times\Omega_2^C} \frac{(\phi_i(x) - \phi_i(y))(\phi_j(x) - \phi_j(y))}{|x-y|^{n+2s_2}}\,\mathrm{dy}\,\mathrm{dx}\,. \end{aligned}$$

The integrals are computed using a composite graded quadrature as standard in boundary element methods [41, Chapter 5]. This method splits the integral into singular and regular parts. It converts the integral over two elements into an integral over $[0,1]^4$ and resolves the singular part with an appropriate grading. The singular part can be computed explicitly, and for the regular part we employ numerical quadrature. The integrals over $\Omega_1^c \cap \Omega_2^c$ can be efficiently computed by numerical quadrature after transforming it to polar coordinates.
The bilinear form for the local problem is implemented in a standard way with the same nodal basis functions $\{\phi_i\}$ of $\mathbb{V}_h$.

In the case of local–nonlocal interface problem we assemble the full Galerkin matrix K from the local and nonlocal components computed over Ω_1, respectively Ω_2. The computations are carried out on quasi-uniform and graded meshes. Graded meshes are designed as discussed in Section 4. First, we use two squares $\Omega_1 = [-1, 0] \times [-0.5, 0.5]$, $\Omega_2 = [0, 1] \times [-0.5, 0.5]$ with the interface $\Gamma = \{0\} \times [-0.5, 0.5]$. We also use Ω a unit disc with $\Omega_1 = B_{1/2}(0)$, $\Omega_2 = B_1(0) \setminus B_{1/2}(0)$ and with the interface $\Gamma = \{(x, y) \in \mathbb{R}^2 | x^2 + y^2 = 1\}$.

8 Numerical experiments for local–nonlocal interface problems

Example 8.1. We consider discretization of the local–nonlocal interface problem, corresponding to (36), in the domain $\Omega = \overline{\Omega_1 \cup \Omega_2}$ where $\Omega_1 = \mathcal{B}_{1/2}$ and $\Omega_2 = \mathcal{B}_1 \setminus \mathcal{B}_{1/2}$. We use algebraically 2–graded meshes graded towards the boundary and the interface $\Gamma = \{(x, y) \in \mathbb{R}^2 | \sqrt{x^2 + y^2} = 1/2\}$. The local part of the problem is solved in Ω_1 and the nonlocal part in Ω_2 for different values of s. We use a forcing function $f = \max\{\exp(-30(x^2 + y^2)) - 0.1, 0\}$ isolated in Ω_1.
The asymptotic behaviour of solutions near the interface for different values of s is summarized in Table 1. Note that the values are in a good agreement with the analytically obtained values. Figure 5 displays asymptotic behaviour of solutions near the interface at the local and nonlocal side for varied values of s.
A numerical solution on a mesh with 39080 elements with $s = 0.7$ is shown in Figure 3.
Figure 4 shows convergence of the energy norm for two distinct values of $s = \frac{3}{10}$ and $s = \frac{7}{10}$ compared to the benchmark solution on the 2-graded mesh. The observed rates for uniform meshes are -0.2399 ($s = \frac{3}{10}$) and -0.245 for ($s = \frac{7}{10}$). For 2-graded meshes we observe rates -0.490 ($s = \frac{3}{10}$) and -0.510 for ($s = \frac{7}{10}$). These closely mirror the approximation results, which predict an approximation error proportional to $DOF^{-1/2}$ on the 2-graded mesh, while the approximation error is $DOF^{-1/4}$ on a uniform mesh.

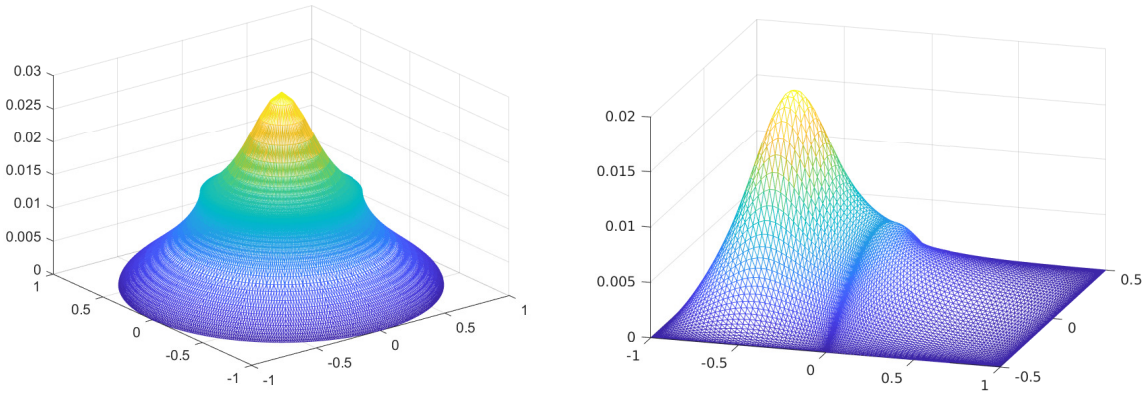

Figure 3: Numerical solution on a mesh with 39080 elements with $s = 0.7$ for the local–nonlocal interface problem in Example 8.1 (left). Numerical solution on a mesh with 16431 elements with f_1 and $s = 0.6$ for the local–nonlocal interface problem in Example 8.2 (right).

Example 8.2. As in Example 8.1 we consider discretization of the local–nonlocal interface problem, corresponding to (36). We consider the domain $\Omega = \overline{\Omega_1 \cup \Omega_2}$ where $\Omega_1 = [-1, 0] \times [-0.5, 0.5]$ and $\Omega_2 = [0, 1] \times [-0.5, 0.5]$. We use algebraically 2–graded meshes with grading towards the boundary and the interface $\Gamma = \{0\} \times [-0.5, 0.5]$. Local part of the problem is solved in Ω_1 while the nonlocal part in Ω_2 for different values of s.

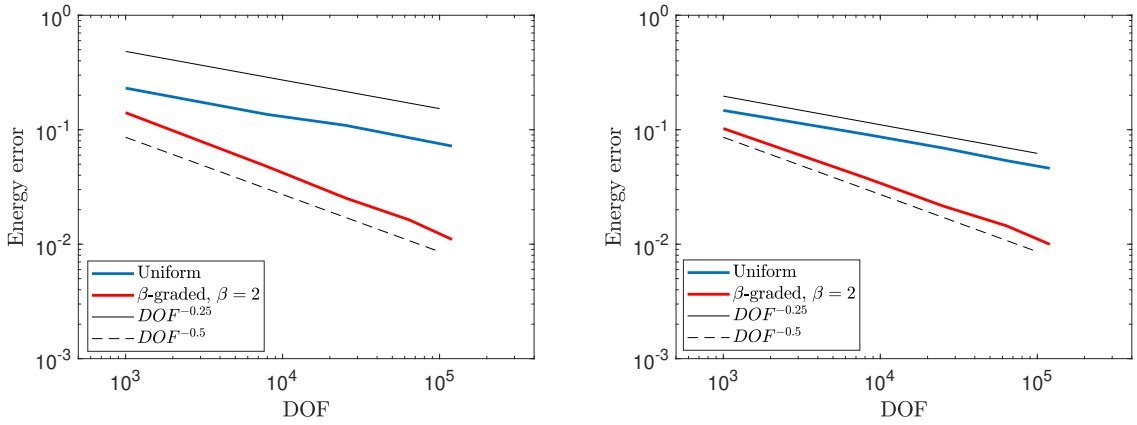

Figure 4: Error in the energy norm for $s = \frac{3}{10}$ (left) and $s = \frac{7}{10}$ (right), Example 8.1.

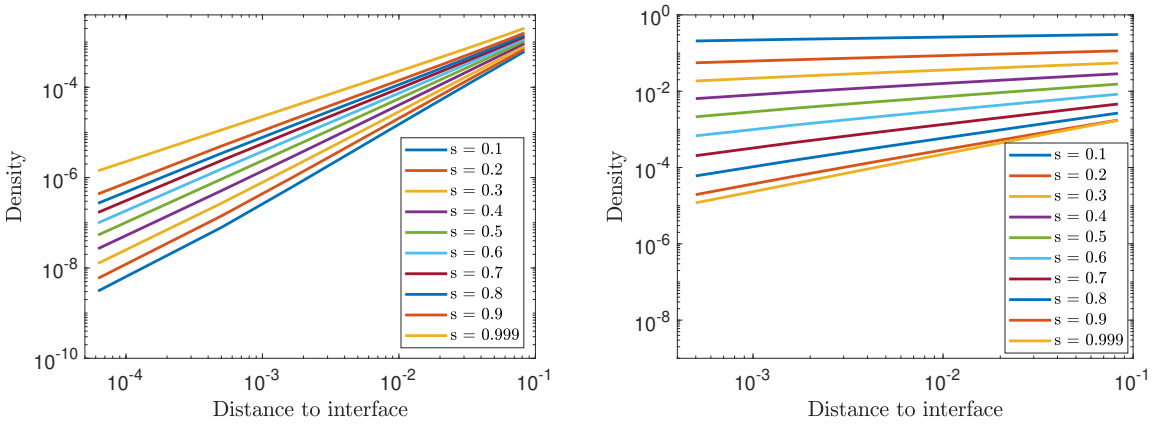

Figure 5: Asymptotic behaviour of the solution near the interface for different values of s and forcing function f in Example 8.1. The slopes are displayed for the local part (left) and the nonlocal part (right).

	s	0.1	0.2	0.3	0.4	0.5	0.6	0.7	0.8	0.9	0.999
Ω_1	$\alpha = 2 - s$	1.82	1.69	1.63	1.51	1.42	1.30	1.25	1.18	1.13	1.01
Ω_2	$\beta = s$	0.09	0.19	0.28	0.37	0.48	0.59	0.71	0.82	0.91	0.98

Table 1: Slopes of the solution in the local, respectively nonlocal part of the domain for variable value of s in Example 8.1. The forcing function $f = \max\{\exp(-30(x^2 + y^2)) - 0.1, 0\}$ is isolated in the local part of the domain away from the interface.

We use two different forcing functions $f_1 = \max\{\exp(-30((x + \frac{1}{2})^2 + y^2)) - 0.1, 0\}$ and $f_2 = \max\{\exp(-30((x - \frac{1}{2})^2 + y^2)) - 0.1, 0\}$ isolated in Ω_1, Ω_2, respectively.
The asymptotic behaviour of solutions near the interface for different values of s and different forcing functions f_1, f_2 is summarized in Tables 2 and 3. The slopes are measured against an extrapolated value of the solution at the interface Γ.
For both forcing functions f_1 and f_2 the values of numerically obtained singular exponents near the interface Γ are in a good agreement with analytically obtained values from Section 6.1 and [5]. Note that the values of the slopes are consistently smaller in Ω_1 due to the effect in

preasymptotic regime coming from the forcing function f_1. However, for f_2 both slopes are in good agreement with theory.
Figures 7 and 8 show the asymptotic behaviour near the interface for the local and nonlocal parts of the domain and for different forcing functions f_1, f_2.
A numerical solution on a mesh with 16431 elements with f_1 and $s = 0.6$ is shown in Figure 3.
Figure 6 shows convergence of the energy norm for two distinct values of $s = \frac{3}{10}$ and $s = \frac{7}{10}$ compared to the benchmark solution on the 2-graded mesh. The observed rates for uniform meshes are -0.252 ($s = \frac{3}{10}$) and -0.249 for ($s = \frac{7}{10}$). For 2-graded meshes we observe rates -0.496 ($s = \frac{3}{10}$) and -0.510 for ($s = \frac{7}{10}$). These closely mirror the approximation results, which predict an approximation error proportional to $DOF^{-1/2}$ on the 2-graded mesh, while the approximation error is $DOF^{-1/4}$ on a uniform mesh.

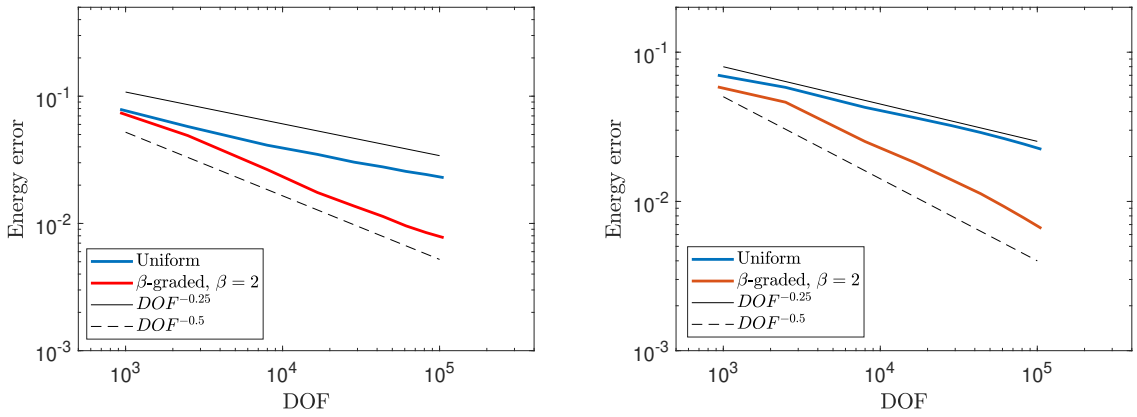

Figure 6: Error in the energy norm for $s = \frac{3}{10}$ (left) and $s = \frac{7}{10}$ (right), Example 8.2.

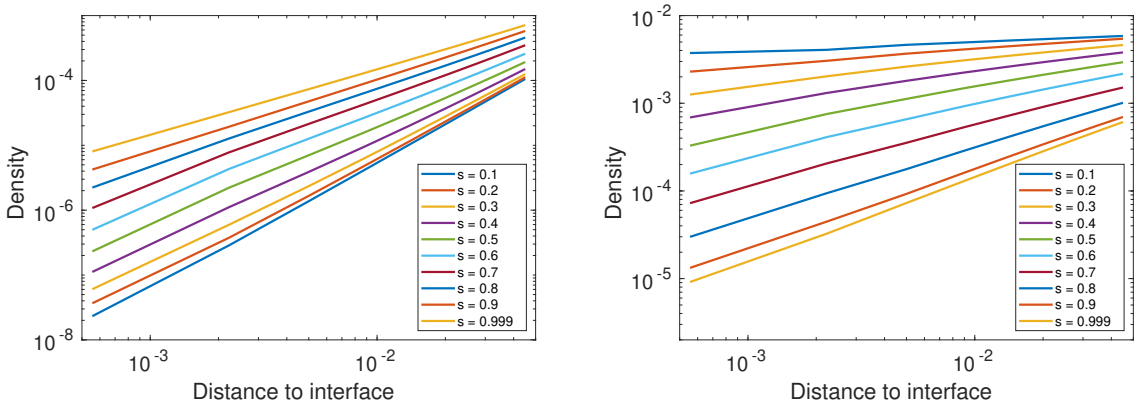

Figure 7: Asymptotic behaviour of the solution near the interface for different values of s and forcing function f_1 in Example 8.2. The slopes are displayed for the local part (left) and the nonlocal part (right).

9 Numerical experiments for nonlocal–nonlocal interface problems

In this section we consider a more general class of interface problems.

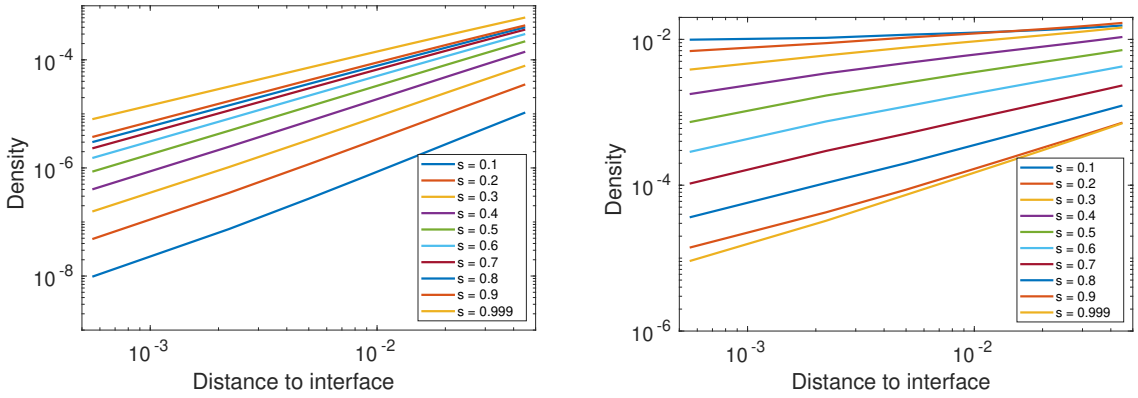

Figure 8: Asymptotic behaviour of the solution near the interface for different values of s and forcing function f_2 in Example 8.2. The slopes are displayed for the local part (left) and the nonlocal part (right).

	s	0.1	0.2	0.3	0.4	0.5	0.6	0.7	0.8	0.9	0.999
Ω_1	$\alpha = 2 - s$	1.73	1.65	1.54	1.44	1.36	1.27	1.21	1.15	1.07	1.00
Ω_2	$\beta = s$	0.11	0.20	0.28	0.37	0.48	0.59	0.72	0.83	0.99	1.00

Table 2: Slopes of the solution in the local, respectively nonlocal part of the domain for variable value of s in Example 8.2. The forcing function $f_1 = \max\{\exp(-30((x+\frac{1}{2})^2 + y^2)) - 0.1, 0\}$ is isolated in the local part of the domain away from the interface.

	s	0.1	0.2	0.3	0.4	0.5	0.6	0.7	0.8	0.9	0.999
Ω_1	$\alpha = 2 - s$	1.93	1.83	1.74	1.62	1.51	1.40	1.30	1.20	1.11	1.01
Ω_2	$\beta = s$	0.10	0.20	0.29	0.39	0.49	0.59	0.69	0.80	0.91	0.99

Table 3: Slopes of the solution in the local, respectively nonlocal part of the domain for variable value of s in Example 8.2. The forcing function $f_2 = \max\{\exp(-30((x-\frac{1}{2})^2 + y^2)) - 0.1, 0\}$ is isolated in the nonlocal part of the domain away from the interface.

Example 9.1. We consider discretization of the nonlocal–nonlocal interface problem corresponding to 30, with $s_1 = s_2$ and different diffusion coefficients $D_1,\ D_2$ in Ω_1 and Ω_2. The domain is given by $\Omega = \overline{\Omega_1 \cup \Omega_2}$ where $\Omega_1 = [-1, 0] \times [-0.5, 0.5]$ and $\Omega_2 = [0, 1] \times [-0.5, 0.5]$. We use algebraically 2–graded meshes with a grading towards both the boundary and the interface $\Gamma = \{0\} \times [-0.5, 0.5]$. We use a forcing function $f = \max\{\exp(-30((x+\frac{1}{2})^2+y^2)) - 0.1, 0\}$. The asymptotic behaviour of solutions near the interface for different values of s and different diffusion coefficients $D_1,\ D_2$ is summarized in Tables 4. The behaviour of numerical solutions near the interface is in good agreement with the analytically obtained values. Note that the values of the slopes are consistently higher in Ω_1 due to the effect in preasymptotic regime coming from the forcing function f.

Figure 11 shows the asymptotic behaviour near the interface for the solution in Ω_2 with $s_1 = s_2 = 0.8$ and $D_1,\ D_2$ varied.

Numerical solutions on a mesh with 25600 elements with f and $s = 0.8$ are shown in Figure 9 for different values of the diffusion coefficient.

Figure 10 shows convergence of the energy norm for $s = \frac{7}{10}$ in both domains with distinct diffusion constant $D_1 = 2$, $D_2 = 1$, and f compared to the benchmark solution on the 2-graded mesh. The observed rates for uniform meshes are -0.2665. For 2-graded meshes we observe

rates -0.5145. These closely mirror the approximation results, which predict an approximation error proportional to $DOF^{-1/2}$ on the 2-graded mesh, while the approximation error is $DOF^{-1/4}$ on a uniform mesh.

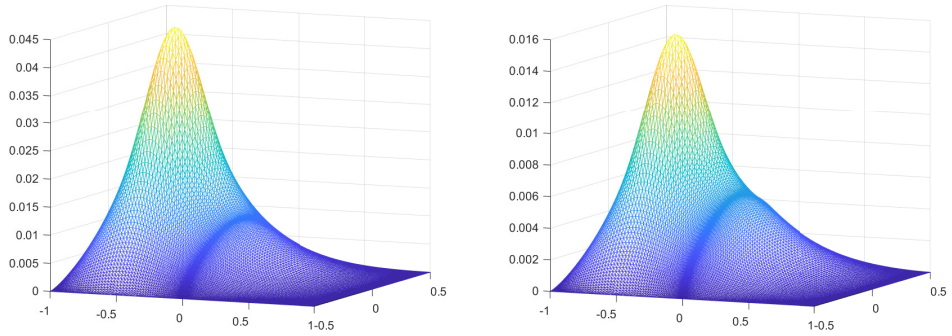

Figure 9: Solutions of the nonlocal-nonlocal interface problem with $s = 0.8$, $D_1 = D_2 = 1$ (left) and $D_1 = 3,\ D_2 = 1$ (right) in Example 9.1.

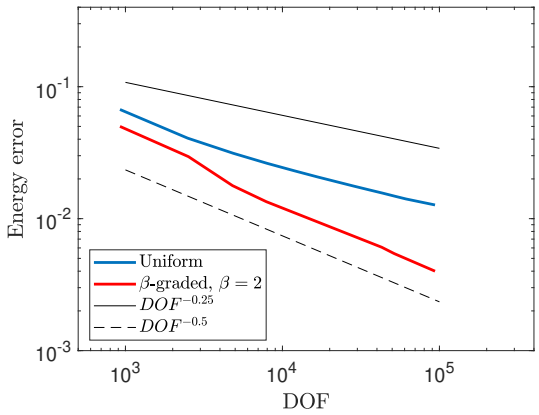

Figure 10: Error in the energy norm for $s = \frac{7}{10}$, $D_1 = 2$, $D_2 = 1$, Example 9.1.

10 Discussion of numerical experiments for different definition of the nonlocal-nonlocal interface problem

Furthermore, we consider a bilinear form introduced in Section 6.4. The bilinear form is implemented in the same way as discussed in Section 7.

Example 10.1. We consider discretization of the nonlocal–nonlocal interface problem corresponding to the bilinear form given by (37). The domain is given by $\Omega = \overline{\Omega_1 \cup \Omega_2}$ where $\Omega_1 = [-1, 0] \times [-0.5, 0.5]$ and $\Omega_2 = [0, 1] \times [-0.5, 0.5]$. We use algebraically 2–graded meshes graded towards the boundary and the interface $\Gamma = \{0\} \times [-0.5, 0.5]$ and a forcing function $f = \max\{\exp(-30((x + \frac{1}{2})^2 + y^2)) - 0.1, 0\}$.

The asymptotic behaviour of solutions near the interface for different values of s is summarized in Tables 5 and 6. The slopes are determined for an extrapolated value of the solution at the interface Γ.

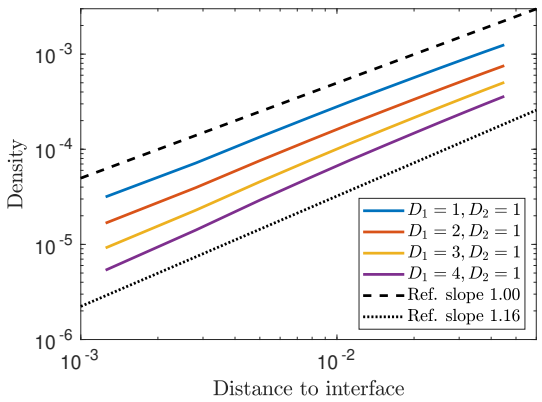

Figure 11: Asymptotic behaviour of the solution near the interface in Ω_2 for different values of D_1, D_2 with $s_1 = s_2 = 0.8$, Example 9.1.

		$s = 0.7$		$s = 0.8$		$s = 0.9$		$s = 0.999$	
Domain	(D_1, D_2)	Num.	Ana.	Num.	Ana.	Num.	Ana.	Num.	Ana.
Ω_1	$(1, 1)$	1.06	1.00	1.08	1.00	1.08	1.00	1.00	1.00
Ω_1	$(2, 1)$	1.11	1.05	1.13	1.04	1.12	1.02	1.03	1.00
Ω_1	$(3, 1)$	1.20	1.17	1.18	1.10	1.14	1.05	1.04	1.00
Ω_2	$(1, 1)$	1.01	1.00	1.02	1.00	1.03	1.00	0.99	1.00
Ω_2	$(2, 1)$	1.05	1.05	1.04	1.04	1.03	1.02	1.00	1.00
Ω_2	$(3, 1)$	1.15	1.17	1.10	1.10	1.06	1.05	1.00	1.00

Table 4: Numerically and analytically obtained values of slopes of the solution in Ω_1, Ω_2 for different values of s in Example 9.1.

The values of numerically obtained singular exponents near the interface Γ are in good agreement with the analytically obtained values in Section 6.4.
The numerical solution on a mesh with f and $s_1 = 0.9$ and $s_2 = 0.5$ is shown in Figure 12. Figure 10 shows the convergence of the energy norm for $s_1 = \frac{7}{10}$ and $s_2 = \frac{1}{2}$ compared to the benchmark solution on the 2-graded mesh. The observed rates for uniform meshes are -0.261. For 2-graded meshes we observe rates -0.501. These closely correspond to the approximation results, which predict an approximation error proportional to $DOF^{-1/2}$ on the 2-graded mesh, while the approximation error is $DOF^{-1/4}$ on a uniform mesh.

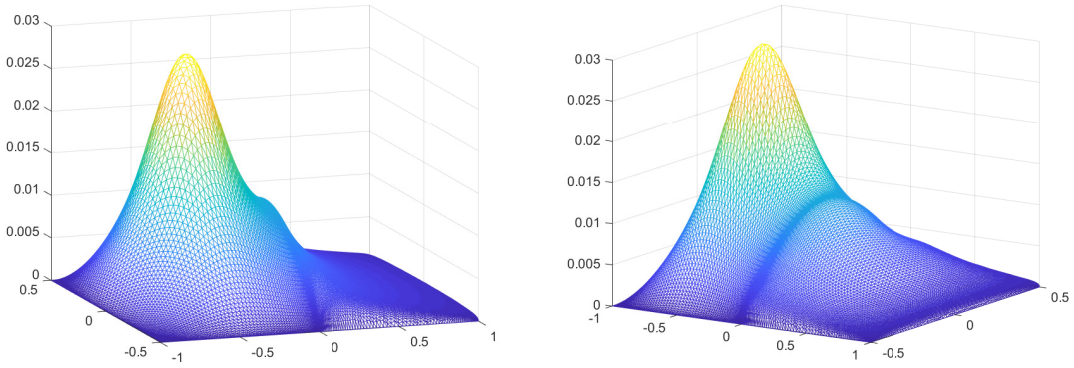

Figure 12: Solution of Example 10.1 for $s_1 = 0.9$ and $s_2 = 0.5$.

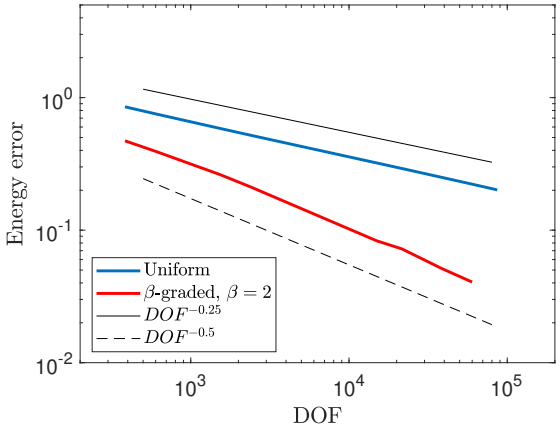

Figure 13: Error in the energy norm for $s_1 = \frac{7}{10}$ and $s_2 = \frac{1}{2}$ on uniform and 2–graded meshes for Example 10.1.

	s_2	0.2	0.3	0.4	0.5	0.6	0.7	0.8	0.9	0.999
Ω_1	$\alpha = 1 + s_1 - s_2$	1.68	1.65	1.55	1.40	1.35	1.28	1.15	1.02	0.901
Ω_2	$\beta = 1 - s_1 + s_2$	0.28	0.42	0.51	0.58	0.69	0.78	0.89	0.98	1.08

Table 5: Behaviour of solutions from Example 10.1 near the interface in Ω_1 and Ω_2, with $s_1 = 0.9$ and s_2 varied.

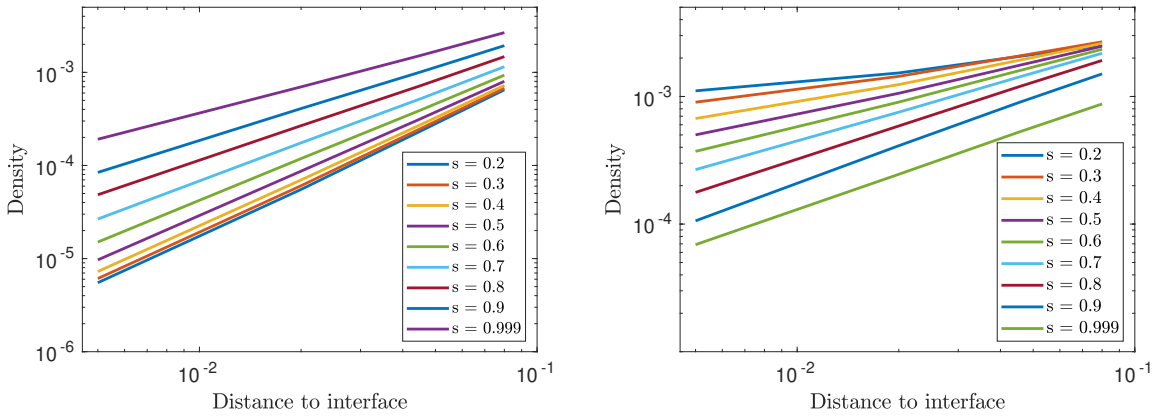

Figure 14: Asymptotic behaviour of solutions near the interface for $s_1 = \frac{9}{10}$ and s_2 varied in Ω_1 (left) and Ω_2 (right) for Example 10.1.

	s_2	0.4	0.5	0.6	0.7	0.8	0.9	0.999
Ω_1	$\alpha = 1 + s_1 - s_2$	1.29	1.21	1.15	1.04	0.96	0.87	0.78
Ω_2	$\beta = 1 - s_1 + s_2$	0.70	0.78	0.89	0.98	1.08	1.19	1.12

Table 6: Behaviour of solutions from Example 10.1 near the interface in Ω_1 and Ω_2, with $s_1 = 0.7$ and s_2 varied.

References

[1] M. D'Elia, M. Perego, P. Bochev, and D. Littlewood, "A coupling strategy for nonlocal and local diffusion models with mixed volume constraints and boundary conditions," *Computers & Mathematics with Applications*, vol. 71, no. 11, pp. 2218–2230, 2016.

[2] K. Zhou and Q. Du, "Mathematical and numerical analysis of linear peridynamic models with nonlocal boundary conditions," *SIAM Journal on Numerical Analysis*, vol. 48, no. 5, pp. 1759–1780, 2010.

[3] E. Madenci and E. Oterkus, *Peridynamic theory and its applications*. Springer, 2016.

[4] J. P. Borthagaray and P. Ciarlet, "Nonlocal models for interface problems between dielectrics and metamaterials," in *2017 11th International Congress on Engineered Materials Platforms for Novel Wave Phenomena (Metamaterials)*, pp. 61–63, IEEE, 2017.

[5] D. Kriventsov, "Regularity for a local–nonlocal transmission problem," *Archive for Rational Mechanics and Analysis*, vol. 217, no. 3, pp. 1103–1195, 2015.

[6] V. Schulz and C. Vollmann, "Shape optimization for interface identification in nonlocal models," *arXiv: 1909.08884*, 2019.

[7] J. Lellmann, K. Papafitsoros, C.-B. Schönlieb, and D. Spector, "Analysis and application of a nonlocal Hessian," *SIAM J. Imaging Sci.*, vol. 8, no. 4, pp. 2161–2202, 2015.

[8] A. Buades, B. Coll, and J.-M. Morel, "A non-local algorithm for image denoising," in *Computer Vision and Pattern Recognition, 2005. CVPR 2005. IEEE Computer Society Conference on*, vol. 2, pp. 60–65, IEEE, 2005.

[9] G. Gilboa and S. Osher, "Nonlocal operators with applications to image processing," *Multiscale Modeling & Simulation*, vol. 7, no. 3, pp. 1005–1028, 2008.

[10] G. Estrada-Rodriguez, H. Gimperlein, K. J. Painter, and J. Stocek, "Space-time fractional diffusion in cell movement models with delay," *Mathematical Models and Methods in Applied Sciences*, vol. 29, no. 01, pp. 65–88, 2019.

[11] G. Estrada-Rodriguez and H. Gimperlein, "Interacting particles with levy strategies: limits of transport equations for swarm robotic systems," *arXiv preprint arxiv:1807.10124*, 2019.

[12] R. Kellogg, "Singularities in interface problems," in *Numerical Solution of Partial Differential Equations–II*, pp. 351–400, Elsevier, 1971.

[13] S. Nicaise, "Polygonal interface problems: higher regularity results," *Communications in Partial Differential Equations*, vol. 15, no. 10, pp. 1475–1508, 1990.

[14] S. Nicaise and A.-M. Sändig, "General interface problems—i," *Mathematical Methods in the Applied Sciences*, vol. 17, no. 6, pp. 395–429, 1994.

[15] B. Guo and E. P. Stephan, "The h-p version of the coupling of finite element and boundary element methods for transmission problems in polyhedral domains," *Numerische Mathematik*, vol. 80, pp. 87–107, Jul 1998.

[16] M. Costabel and E. Stephan, "A direct boundary integral equation method for transmission problems," *Journal of Mathematical Analysis and Applications*, vol. 106, no. 2, pp. 367 – 413, 1985.

[17] H. Gimperlein, E. Stephan, and J. Stocek, "Corner singularities for the fractional laplacian and finite element approximation.," *in preparation*, 2019.

[18] J. C. Dallon and J. A. Sherratt, "A mathematical model for spatially varying extracellular matrix alignment," *SIAM Journal on Applied Mathematics*, vol. 61, no. 2, pp. 506–527, 2000.

[19] A. Chauviere, T. Hillen, and L. Preziosi, "Modeling cell movement in anisotropic and heterogeneous network tissues," *Networks and heterogeneous media*, vol. 2, no. 2, p. 333, 2007.

[20] S. Fedotov, "Nonlinear subdiffusive fractional equations and the aggregation phenomenon," *Physical Review E*, vol. 88, no. 3, p. 032104, 2013.

[21] A. Giese, L. Kluwe, B. Laube, H. Meissner, M. E. Berens, and M. Westphal, "Migration of human glioma cells on myelin," *Neurosurgery*, vol. 38, no. 4, pp. 755–764, 1996.

[22] A. Boissonnas, L. Fetler, I. S. Zeelenberg, S. Hugues, and S. Amigorena, "In vivo imaging of cytotoxic t cell infiltration and elimination of a solid tumor," *Journal of Experimental Medicine*, vol. 204, no. 2, pp. 345–356, 2007.

[23] T. H. Harris, E. J. Banigan, D. A. Christian, C. Konradt, E. D. T. Wojno, K. Norose, E. H. Wilson, B. John, W. Weninger, A. D. Luster, *et al.*, "Generalized lévy walks and the role of chemokines in migration of effector cd8+ t cells," *Nature*, vol. 486, no. 7404, p. 545, 2012.

[24] F. R. Macfarlane, T. Lorenzi, and M. A. Chaplain, "Modelling the immune response to cancer: an individual-based approach accounting for the difference in movement between inactive and activated t cells," *Bulletin of mathematical biology*, vol. 80, no. 6, pp. 1539–1562, 2018.

[25] J. R. Potts, G. Bastille-Rousseau, D. L. Murray, J. A. Schaefer, and M. A. Lewis, "Predicting local and non-local effects of resources on animal space use using a mechanistic step selection model," *Methods in Ecology and Evolution*, vol. 5, no. 3, pp. 253–262, 2014.

[26] J. R. Potts, T. Hillen, and M. A. Lewis, "The "edge effect" phenomenon: deriving population abundance patterns from individual animal movement decisions," *Theoretical Ecology*, vol. 9, no. 2, pp. 233–247, 2016.

[27] B. Berkowitz, A. Cortis, M. Dentz, and H. Scher, "Modeling non-fickian transport in geological formations as a continuous time random walk," *Reviews of Geophysics*, vol. 44, no. 2, 2006.

[28] Y. Zhang, E. M. LaBolle, and K. Pohlmann, "Monte Carlo simulation of superdiffusion and subdiffusion in macroscopically heterogeneous media," *Water Resources Research*, vol. 45, no. 10, 2009.

[29] S. Dipierro, X. Ros-Oton, and E. Valdinoci, "Nonlocal problems with neumann boundary conditions," *Revista Matemática Iberoamericana*, vol. 33, no. 2, pp. 377–416, 2017.

[30] T. Hillen and K. J. Painter, "Transport and anisotropic diffusion models for movement in oriented habitats," in *Dispersal, individual movement and spatial ecology*, pp. 177–222, Springer, 2013.

[31] H. G. Othmer, S. R. Dunbar, and W. Alt, "Models of dispersal in biological systems," *Journal of Mathematical Biology*, vol. 26, no. 3, pp. 263–298, 1988.

[32] G. Estrada-Rodriguez, H. Gimperlein, and K. J. Painter, "Fractional Patlak–Keller–Segel equations for chemotactic superdiffusion," *SIAM Journal on Applied Mathematics*, vol. 78, no. 2, pp. 1155–1173, 2018.

[33] M. M. Meerschaert, J. Mortensen, and S. W. Wheatcraft, "Fractional vector calculus for fractional advection–dispersion," *Physica A: Statistical Mechanics and its Applications*, vol. 367, pp. 181–190, 2006.

[34] M. D'Ovidio, R. Garra, *et al.*, "Multidimensional fractional advection-dispersion equations and related stochastic processes," *Electronic Journal of Probability*, vol. 19, 2014.

[35] M. Felsinger, M. Kassmann, and P. Voigt, "The dirichlet problem for nonlocal operators," *Mathematische Zeitschrift*, vol. 279, pp. 779–809, Apr 2015.

[36] G. Grubb, "Fractional laplacians on domains, a development of hörmander's theory of μ-transmission pseudodifferential operators," *Advances in Mathematics*, vol. 268, pp. 478 – 528, 2015.

[37] T. von Petersdorff, "Randwertprobleme der elastizitätstheorie für polyeder-singularitäten und approximation mit randelementmethoden," *Ph.D. thesis, Technische Universität Darmstadt*, 1989.

[38] G. Acosta, F. M. Bersetche, and J. P. Borthagaray, "A short FE implementation for a 2d homogeneous Dirichlet problem of a fractional Laplacian," *Computers and Mathematics with Applications*, vol. 74, no. 4, pp. 784 – 816, 2017.

[39] M. Ainsworth and C. Glusa, "Aspects of an adaptive finite element method for the fractional Laplacian: a priori and a posteriori error estimates, efficient implementation and multigrid solver," *Computer Methods in Applied Mechanics and Engineering*, vol. 327, pp. 4–35, 2017.

[40] H. Gimperlein and J. Stocek, "Space–time adaptive finite elements for nonlocal parabolic variational inequalities," *Computer Methods in Applied Mechanics and Engineering*, vol. 352, pp. 137 – 171, 2019.

[41] S. A. Sauter and C. Schwab, *Boundary element methods*, vol. 39 of *Springer Series in Computational Mathematics*. Springer-Verlag, Berlin, 2011.